

## Far-infrared spectroscopy of PbTe doped with iron

P. M. NIKOLIĆ<sup>1</sup>, K. RADULOVIĆ<sup>1</sup>, D. VASILJEVIĆ-RADOVIĆ<sup>1</sup>, V. BLAGOJEVIĆ<sup>2</sup>,  
B. MILOSAVLJEVIĆ<sup>3</sup> and Z. DOHČEVIĆ-MITROVIĆ<sup>4</sup>

<sup>1</sup>Institute of Technical Science of SASA, P. O. Box 315, YU-11000 Belgrade, <sup>2</sup>Faculty of Electrical Engineering, Belgrade University, P. O. Box 35-54, YU-11120 Belgrade, <sup>3</sup>Institute of Copper, Department for Chemical and Technical Control, Bor and <sup>4</sup>Institute of Physics, P. O. Box 75, YU-11000 Belgrade, Yugoslavia

(Received 26 February 2002)

Far infrared reflection spectra, at room and liquid nitrogen temperature, of PbTe single crystals doped with iron are presented. Plasma minima were observed at about  $160\text{ cm}^{-1}$  and  $180\text{ cm}^{-1}$  for room and liquid nitrogen temperature, respectively. Using the reflectivity diagrams and their minima, the values of the hole concentrations and their mobility at both temperatures were calculated and compared with galvanomagnetic measurements. All these results indicated that when PbTe is doped with a small concentration of Fe, the hole concentration is reduced by one order of magnitude and the free carrier mobility is larger when compared to pure PbTe.

*Keywords:* lead telluride, doped, infrared spectroscopy, plasma.

### INTRODUCTION

In a number of scientific groups all over the world, special attention has been paid to investigations of impurity states of IV-VI narrow gap semiconductors based on lead telluride.<sup>1–5</sup>

Lead telluride and lead-tin-telluride are well-known materials used for the production of lasers and LEDs working in the IR and FIR ranges.<sup>6</sup> Improvement of their properties could be very useful for practical applications and this can be attained by doping.

The introduction of an impurity results in the appearance of a deep energy level with a high density of states which exhibits quite unusual properties, such as Fermi level pinning,<sup>7</sup> persistent photoconductivity,<sup>8</sup> etc. The position of the impurity level has been studied for various compositions, temperatures and magnetic fields for different alloys and dopants: PbTe(B),<sup>4</sup> PbTe(In), PbTe(Ga),<sup>9</sup> PbTe(Cr), PbTe(Yb),<sup>10</sup> PbTe(Pt),<sup>11</sup>  $\text{Pb}_{1-x}\text{Sn}_x\text{Te}(\text{In}, \text{Ga})$ ,  $\text{Pb}_{1-x}\text{Mn}_x\text{Te}(\text{In}, \text{Ga})$ ,<sup>12</sup> PbTe(Ce).<sup>13</sup>

Doping IV-VI alloys with magnetic impurities provides a modification of the semiconductor energy spectrum in a magnetic field. Some dopants (Eu, Mn) modify the energy spectrum of a host semiconductor material. They are most commonly used for the forma-

tion of barrier spacers in IV-VI heterostructures, where the barrier parameters depend on the magnetic field. Other impurities such as Yb and Cr form impurity levels in the proximity of the actual bands. In this case, the position of the pinned Fermi level may be tuned by variation of a magnetic field. These results open new possibilities for the construction of a magnetic field tunable photovoltaic infrared photodetector.

To the best of our knowledge, PbTe doped with iron has not yet been studied although the effects of other transition metals (Cr, Yb and Pt) have been studied.

#### EXPERIMENTAL

A single crystal ingot of PbTe doped with Fe was grown by the classical Bridgman method using elements of high purity (6N) as source materials. The concentration of Fe in the melt corresponded to the doping level of 3 at. % Fe. Freshly cleaved samples were used for reflectivity measurements. The content of iron in each sample was determined by ICP and EDS analyses. The factor of segregation of Fe in PbTe was  $\ll 1$ , so the majority of samples had a small content of Fe, between 0.026 at. % and 0.16 at. %. All samples were of the p type. The far infrared reflection spectra at room, and liquid nitrogen temperatures, were measured using a BOMEM Fourier Transform Spectrometer. Experimental reflectivity diagrams, measured at 300 K and 80 K, versus the wave number, are given in Fig. 1 and Fig. 2 respectively. The content of iron in this sample, which was located in the middle of the ingot, was about 0.04 at. %.

#### RESULTS AND DISCUSSION

The experimental reflectivity data were numerically analyzed. In both cases the pure LO-mode of the host lattice is strongly influenced by the plasmon mode ( $\omega_p$ ) of the free carrier. As a result, a combined plasmon-LO phonon mode should be observed. The numerical analysis of the experimental data was done using the dielectric function which takes into account the existence of a plasmon-LO phonon interaction:<sup>14</sup>

$$\varepsilon(\omega) = \varepsilon_\infty \frac{\prod_{j=1}^2 (\omega^2 + i\gamma_{lj}\omega - \omega_{lj}^2)}{\omega(\omega + i\gamma_p)(\omega^2 + i\gamma_t\omega - \omega_t^2)} \prod_{n=1}^p \frac{(\omega^2 + i\gamma_{lon}\omega - \omega_{lon}^2)}{(\omega^2 + i\gamma_{ton}\omega - \omega_{ton}^2)} \prod_{k=1}^r \frac{(\omega^2 + i\gamma_{LOk}\omega - \omega_{LOk}^2)}{(\omega^2 + i\gamma_{TOk}\omega - \omega_{TOk}^2)} \quad (1)$$

The  $\omega_{lj}$  and  $\gamma_{lj}$  parameters of the first numerator represent eigen frequencies and damping factors of the longitudinal plasmon-phonon waves, respectively, which arise as a result of the interaction of the initial modes.  $\omega_t$  and  $\gamma_t$  are the frequency and damping factor of the transverse phonon mode;  $\gamma_p$  is the damping factor of the plasmon, and  $\varepsilon_\infty$  is the high frequency dielectric permittivity. The second term in Eq. (1) represents the local modes of the Fe impurity. In the third term, which corresponds to uncoupled modes of the host crystal,  $\omega_{LOk}$  and  $\omega_{TOk}$  are the longitudinal and transverse frequencies,  $\gamma_{LOk}$  and  $\gamma_{TOk}$  are damping factors.

Eq. (1) can be used in the case of paired coupled plasma-LO phonon modes to obtain the frequencies of the experimental coupled modes ( $\omega_{11}$ ,  $\omega_{12}$ ). The values of  $\omega_p$ , for room and liquid nitrogen temperature, are obtained from Eq. (2):

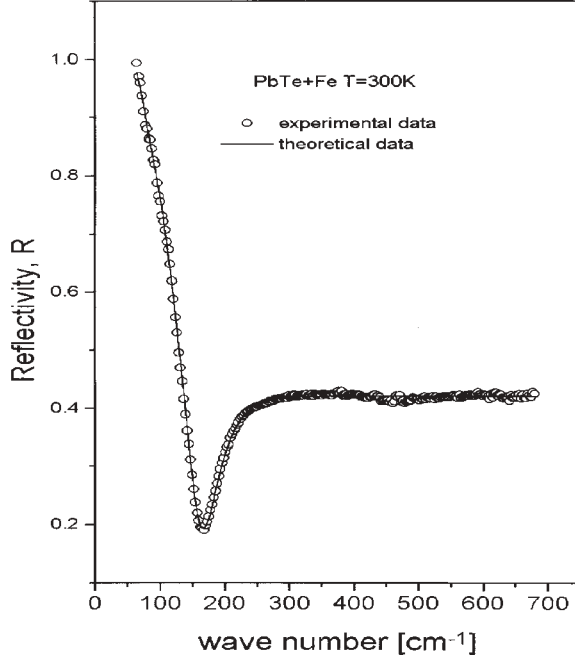


Fig. 1. Room temperature reflectivity spectra of a PbTe+Fe single crystal. Experimental results are presented by circles. The solid line is the theoretical curve obtained by a fitting procedure using Eq. (1).

$$\omega_{11}\omega_{12} = \omega_p\omega_t \quad (2)$$

Then Eq. (3) is used to calculate the effective mass of the free carriers.

$$\omega_p = \sqrt{\frac{Pe^2}{\epsilon_0\epsilon_\infty m^*}} \quad (3)$$

$P$  is the free carrier concentration (hole in our sample);  $e$  is the magnitude of the electron charge;  $\epsilon_0$  and  $\epsilon_\infty$  are the dielectric permittivity of vacuum and at the high frequency range where the optical reflectivity was measured, respectively;  $m^*$  is the effective mass of the free holes.

The literature reflectivity data given by Dixon and Riedl<sup>15</sup> and Boss and Kinch<sup>16</sup> for p type PbTe samples were used in this work. The values of the carrier concentration, and their plasma wavelength values are given in Table I.

Using literature data, a diagram of  $P$  versus the plasma wavelength was constructed in a log-log scale (Fig. 3). In this way, using this diagram and reflectivity minima at about 160  $\text{cm}^{-1}$  for room temperature and about 180  $\text{cm}^{-1}$  for liquid nitrogen temperature, the values of the hole concentrations at the sample were determined as  $P_{80\text{K}} \approx 3 \times 10^{17} \text{ cm}^{-3}$  and  $P_{300\text{K}} \approx 2.4 \times 10^{17} \text{ cm}^{-3}$ . Using these values, the room temperature and 80 K effective mass  $m_{300\text{K}} \approx 0.04m_0$  and  $m_{80\text{K}} \approx 0.033m_0$  were calculated. If these values are compared with literature data for a pure p type PbTe,  $m^* = 0.02 m_0$  for light holes and  $m^* = 0.31 m_0$  for heavy holes, it can be concluded that the carrier concentration for these samples was significantly decreased, because the Fermi level was pinned in the valence band at the position of the light holes.

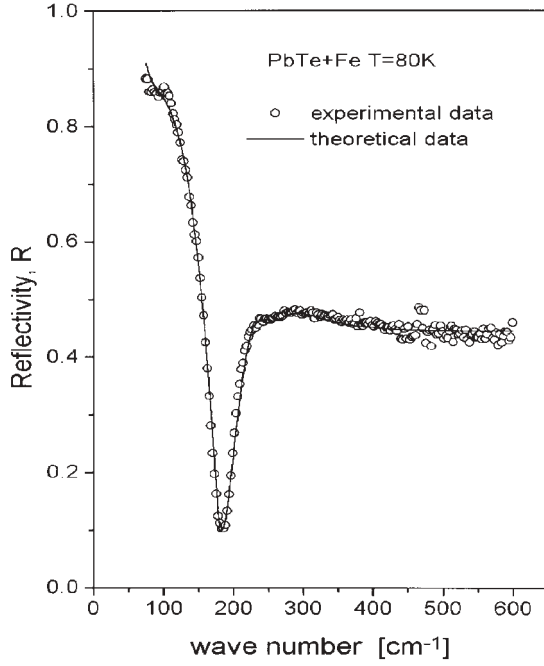


Fig. 2. Reflectivity spectra of PbTe+Fe single crystal at 80 K. Experimental results are presented by circles. The solid line is obtained by a fitting procedure.

TABLE I. The values of carrier concentration and plasma wavelength values

Sample	Reference	Carrier concentration [cm <sup>-3</sup> ]	Plasma minimum wavelength [μm]
A	15	$3.5 \times 10^{18}$	23.5
B	15	$5.7 \times 10^{18}$	20
C	15	$1.5 \times 10^{19}$	15
D	15	$4.8 \times 10^{19}$	9
E	16	$3 \times 10^{17}$	52.6

This can be explained by the displacement of the band edges of PbTe with temperature. In Fig. 4 (Ref. 17) the band edge structure of PbTe is given, where the inversion of the valence band, at about 450 °C, can be seen. The presence of two valence bands is obvious and at low temperatures the light hole valence band is much nearer the bottom of the conduction band and at those temperatures the energy gap decreases.

This analysis could be extended using the following equations: <sup>18</sup>

$$\varepsilon_1(\omega) = n^2 - k^2 = \varepsilon_\infty - \frac{Pe^2}{m^* \varepsilon_0} \frac{\tau^2}{1 + \omega^2 \tau^2}$$

$$\varepsilon_2(\omega) = 2nk\omega = \frac{Pe^2}{m^* \varepsilon_0} \frac{\tau}{1 + \omega^2 \tau^2}$$

$$R = \frac{(n-1)^2 + k^2}{(n+1)^2 + k^2}$$

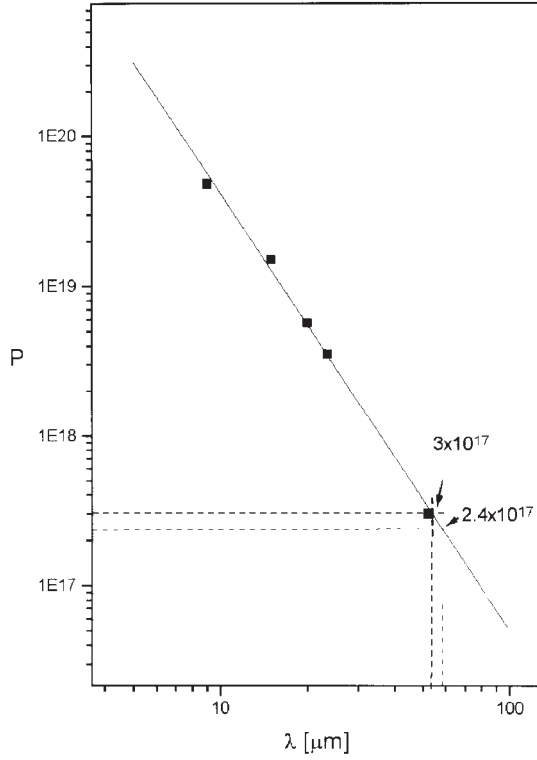


Fig. 3. Free hole concentrations  $P$  versus plasma wavelength for PbTe.

Using these equations, it can easily be determined that for  $\omega^2\tau^2 \gg 1$  and  $n^2 \gg k^2$ .

$$n^2 = \epsilon_\infty - \frac{Pe^2}{m^* \epsilon_0 \omega^2} = \epsilon_\infty \left( 1 - \frac{\omega_p^2}{\omega^2} \right) \quad \text{and}$$

$$\frac{\omega_p}{\omega_{\min}^2} = 1 - \frac{n_{\min}^2}{\epsilon_\infty}$$

$$\tau\omega_{\min} = \frac{\epsilon_\infty - n_{\min}^2 + k_{\min}^2}{2n_{\min} k_{\min}}$$

General diagrams for  $\tau\omega_{\min} = \varphi(R_{\min})$ , when  $\sqrt{\epsilon_\infty}$  is a parameter, can be calculated using the Moss *et al.* method<sup>18</sup> and are given in Fig. 5.

Using this diagram, the values of  $\tau\omega_{\min(300K)} = 3.95$ ,  $\tau\omega_{\min(80K)} = 8.96$ , and finally  $\tau_{300K} = 1.29 \times 10^{-13}$  s,  $\tau_{80K} = 3.4 \times 10^{-13}$  s have been determined. The mobility values for the free carriers were calculated as  $\mu_p \approx \frac{e\tau}{m^*}$ ,  $\mu_{p80} \approx 181.38$  cm<sup>2</sup>/Vs,  $\mu_{p300} \approx 5485$  cm<sup>2</sup>/Vs.

It is interesting to see the difference if PbTe is doped with some other transition metals. Mn and Cr are the nearest to iron in the periodic system. In both cases, the plasma fre-

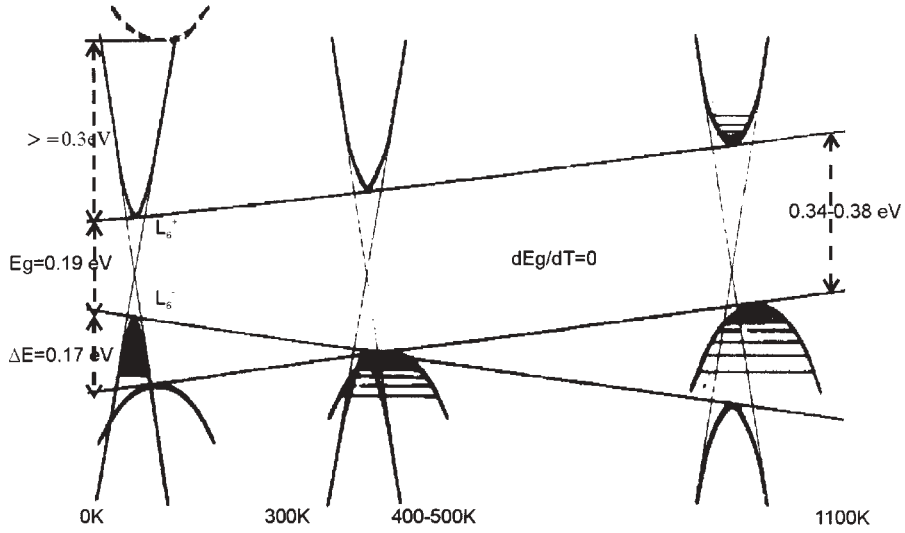


Fig. 4. The band structure of PbTe with inversion of the valence band at about 450 °C.

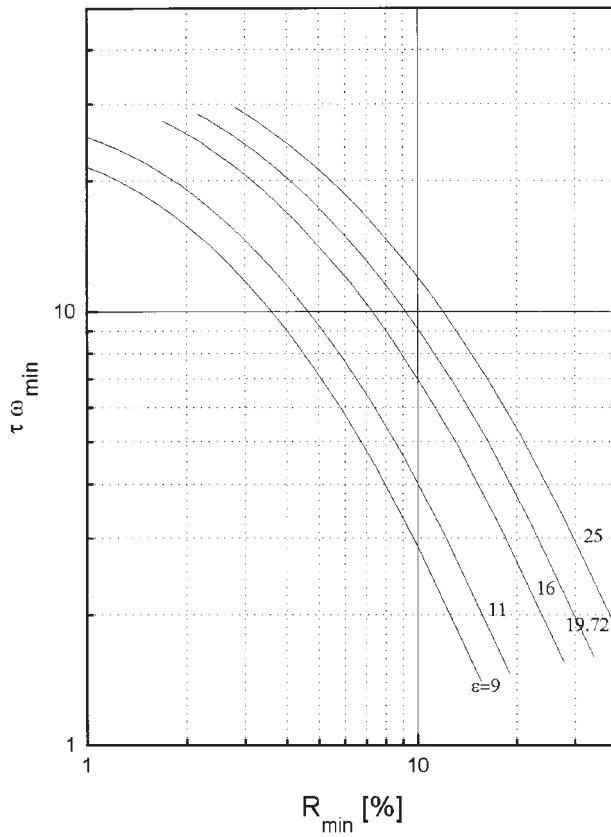


Fig. 5. General diagrams for  $\tau \omega_{\min} = \varphi(R_{\min})$  where  $\epsilon_{\infty}$  is a parameter.

quency decreases when the content of either Mn or Cr is increased from a very low value to about 0.2 at%. When PbTe is doped with Fe, the plasma frequency increases when the temperature is decreased from room temperature, similar to the case when PbTe is doped with Mn or Cr.

Numerical analyses of both the room temperature and 80 K reflectivity diagrams, given in Figs. 1 and 2, were done using a fitting procedure of the experimental results with the theoretical curve given by Eq. 1. The solid lines in Figs. 1 and 2 are calculated spectra obtained by the fitting procedure. Some calculated parameters are given in Table II, where  $\omega_p$  is the plasma frequency, " $g_p$ " its damping factor and  $\epsilon_\infty$  is the high frequency dielectric permittivity.

The damping factor  $g_p$  at 80 K is much smaller compared with the values for room temperature. At the same time, the value of the high frequency dielectric permittivity increases and the plasma frequency damping factor decreases with decreasing temperature. This is expected, judging by the much sharper reflectivity minimum when the temperature is decreased. In the fitting procedure a transverse phonon frequency, at about  $34 \text{ cm}^{-1}$  was also determined (Ref. 20) then an oscillation of a weak intensity at about  $84 \text{ cm}^{-1}$  which belongs to a mode from the edge of the Brillouin zone. A longitudinal mode of pure PbTe at about  $105 \text{ cm}^{-1}$  was also obtained, which is in reasonable agreement with the previously mentioned literature data.

TABLE II. Calculated parameters for PbTe doped with Fe

Temperature	$\omega_p/\text{cm}^{-1}$	$g_p/\text{cm}^{-1}$	$\epsilon_\infty$
300 K	162	45	21.9
80 K	181	25	25

The local mode of iron is observed at about  $270 \text{ cm}^{-1}$  only at 80 K and another feature at about  $450 \text{ cm}^{-1}$ . The local modes for iron could belong to one of several electron states:  $\text{Fe}^{2+}$ ,  $\text{Fe}^{3+}$  or  $\text{Fe}^+$ . One can expect that the  $\text{Fe}^+$  electron state is a more stable state than the metastable electron state  $\text{Fe}^{2+}$  or the empty state  $\text{Fe}^{3+}$ . The position of the pinned Fermi level is defined by the balance between  $\text{Fe}^+$  and  $\text{Fe}^{3+}$  charge impurity states. We believe that the Fermi level is pinned near the top of the valence band and the sample is p-type.

## CONCLUSION

Single crystal samples of lead telluride doped with iron were made and the far infrared reflectivity spectra were measured at room temperature and at about 80 K. A plasma minimum in both cases was observed at rather low frequency. It indicated that, when PbTe is doped with Fe, the carrier concentration decreases. The calculated values for the hole concentration confirmed that the free hole concentration was by one order of magnitude smaller for PbTe doped with Fe when compared with single crystals of pure PbTe.

It is supposed that iron as a dopant behaves in a similar manner to the elements of the IIIA group when PbTe was doped with In or B.

## ИЗВОД

ОПТИЧКА СВОЈСТВА РbTe ДОПИРАНОГ ГВОЖЂЕМ У ДАЛЕКОЈ  
ИНФРАЦРВЕНОЈ ОБЛАСТИ

П. М. НИКОЛИЋ<sup>1</sup>, К. РАДУЛОВИЋ<sup>1</sup>, Д. ВАСИЉЕВИЋ-РАДОВИЋ<sup>1</sup>, В. БЛАГОЈЕВИЋ<sup>2</sup>,  
Б. МИЛОСАВЉЕВИЋ<sup>3</sup> и З. ДОХЧЕВИЋ-МИТРОВИЋ<sup>4</sup>

<sup>1</sup>Институт за техничке науке САНУ, б. бр. 315, 11000 Београд, <sup>2</sup>Електротехнички факултет, Универзитет у Београду, б. бр. 3554, 11120 Београд, <sup>3</sup>Институт за бакар, Одсек за хемијску и техничку контролу, Бор и <sup>4</sup>Институт за физику, б. бр. 75, 11000 Београд

Приказани су рефлексциони оптички спектри за монокристални олово-телурид, снимљени у далекој инфрацрвеној области. Плазма-минимум посматран је на око 160 cm<sup>-1</sup> и 180 cm<sup>-1</sup> на собној температури и на температури течног азота, респективно. Концентрације слободних носилаца – шупљина и њихове покретљивости израчунате су за обе температуре коришћењем рефлексционих дијаграма. Добијене вредности су упоређиване са галваномagnetним мерењима. Добијени резултати показују да је концентрација шупљина у РbTe допираном малом концентрацијом Fe, смањена за ред величине и да је њихова покретљивост већа у поређењу са чистим РbTe.

(Примљено 26. фебруара 2002)

## REFERENCES

1. B. A. Akimov, V. N. Shumskiy, O. I. Petikov, *Infrared Physic* **34** (1993) 375
2. S. N. Chesnokov, D. E. Dolzherko, I. I. Ivanchik, D. M. Khokhlov, *Infrared Physic Technology* **35** (1994) 23
3. N. Romčević, Z. V. Popović, D. M. Khoklov, W. König, *Infrared Physics and Technology*, **40** (1999) 453
4. P. M. Nikolić, N. Romčević, K. Radulović, S. S. Vujatović, S. Đurić, V. Blagojević, P. Mihajlović, D. Siapakas, T. T. Zorba, *Science of Sintering* **31** (1999) 125
5. S. Takaoka, T. Hamaguchi, S. Shimomura, K. Murase, *Solid St. Comm.* **V54** (1985) 99
6. H. Zogg, C. Maissen, J. Masek, T. Hoshino, S. Blunier, A. N. Tiwari, *Semicond. Sci. Technology* **6** (1991) C36
7. J. Niewodniezanska-Zawadzka, A. Szczerbakow, *Solid St. Comm.* **34** (1980) 887
8. N. Ž. Romčević, Z. V. Popović, D. R. Khokhlov, W. König, *Infrared Physic* **38** (1997) 117
9. N. Romčević, M. Romčević, D. R. Khokhlov, I. I. Ivanchik, in *High Temperature Superconductor and Novel Inorganic Materials*, Van Tendelov Eds., (1997) p. 297
10. B. A. Akimov, P. V. Verteletski, V. P. Zlomanov, L. I. Ryabova, O. I. Tananaeva, N. A. Shirokova, *Sov. Phys. Semicond.* **23** (1989) 11
11. P. M. Nikolić, M. B. Pavlović, S. S. Vujatović, *Infrared Physic* **26** (1986) 5
12. B. A. Akimov, A. V. Nikorich, L. I. Ryabova, N. A. Shirokova, *Sov. Phys. Semicond.* **23** (1989) 636
13. P. M. Nikolić, K. T. Radulović, S. S. Vujatović, D. Vasiljević-Radović, S. Đurić, V. Blagojević, P. Mihajlović, D. Urošević, Z. Dohčević-Mitrović, O. Jakšić, *J. Optoelectronic and Advanced Materials*, **2** (2000) 465
14. A. A. Kuhkarskii, *Solid State Commun.* **13** (1973) 1761
15. J. R. Dixon, H. R. Riedl, *Phys. Rev.* **V138, N3A, A873** (1965)
16. D. D. Buss, M. A. Kinch, *Proceed. Phys. of IV-VI Compounds and Alloys*, Pennsylvania (1972) p. 209
17. A. A. Andreev, *J. de Physique Coll.* **C4** (1968) 50

18. T. S. Moss, *Optical Properties of Semiconductors*, A Semiconductor Monograph Butterworth, London (1959)
19. T. S. Moss, T. D. F. Howkins, G. J. Burrell, *J. Phys. C*, **1** (1968) 1435
20. Yu. Ravich, B. A. Efimova, T. A. Smirnov, *Semiconducting Lead Chalcogenide*, L. S. Stil, Ed., Plenum Press, New York (1970).